Particle transport and flow modification in planar temporally evolving mixing layers. II. Flow modification due to two-way coupling

Chidambaram Narayanan[a] and Djamel Lakehal[b]
Institute of Energy Technology, Swiss Federal Institute of Technology, ETH-Zentrum/CLT, CH-8092 Zurich, Switzerland

(Received 1 December 2005; accepted 31 July 2006; published online 14 September 2006)

Simulations of two-dimensional, two-way coupled particle-laden mixing layers were performed for particles with various Stokes numbers, at mass loadings between 0.1 and 0.5. This component complements Part I of the study, where particle and fluid transport was analyzed under one-way coupling. Under two-way coupling, the accumulation of particles in the periphery of the Kelvin-Helmholtz vortices results in the formation of intricate undulating patterns, and rupture and break-up of the vortices. At higher mass loadings the vortex structure is completely destroyed. The overall accumulation at the edges of the mixing layer is significantly reduced due to two-way coupling. The rate of evacuation of the vortex core was found to be much slower compared to one-way coupling. In a global sense, particles delay the development of the mixing layer in terms of saturation of the fundamental and the subharmonic modes. Significant generation of small-scale vorticity and higher energy in the small scales is observed at higher mass loadings. Particles are shown to increase the modal kinetic energy dissipation rate. The mean fluid kinetic energy balance shows that most of the kinetic energy exchange between the particle and fluid phases takes place at the edges of the mixing layer. As the mixing layer evolves, the kinetic energy exchange with the particle phase was shown to decrease in importance compared to the other terms in the mean kinetic energy balance; namely, the energy exchange between the mean and the modal fields and the modal transport term. © *2006 American Institute of Physics*. [DOI: 10.1063/1.2352730]

I. INTRODUCTION

In Part I of this study, particle transport in a two-dimensional mixing layer was analyzed under the condition of one-way coupling. However, in most practical particulate flows, the effect of particles on the flow dynamics is of critical importance. In this part, the two-way coupled particle-laden mixing layer problem is analyzed. The two-dimensional, two-way coupled, particle-laden mixing layer problem can be split into two parts. The first one deals with how the linear stability of the flow is altered by the particle phase.[1,2] The results of the linear stability analysis provide the most unstable wavenumbers for different particle Stokes numbers and mass loadings. The second issue is how particles affect the later evolution of the mixing layer, which includes the roll-up of strong spanwise vortices and their eventual pairing to form one large vortex. There have been relatively fewer studies on this aspect. The present contribution aims at shedding light on the effect of the two-way interaction on fluid momentum transport mechanisms and particle transport.

Druzhinin[3] considered particle accumulation and flow modulation in several types of flows representing steady solutions of the two-dimensional Euler equations, including flow in an elliptical stagnation point, in the vicinity of a hyperbolic stagnation point, in a circular vortex and in a Stuart vortex. Analytical and numerical solutions obtained showed that owing to two-way coupling, the vorticity in the centers of the vortices is reduced, while the strain rate in the braid region is enhanced. At the locations of concentration *sheets*, gradients of the fluid velocity are increased because of the drag forces between the two phases, and sheets of increased vorticity are formed.

Wang *et al.*[4] studied the flow modulation of two-dimensional temporally evolving mixing layers by particles. They used an Eulerian-Eulerian method and studied the effect of particles with Stokes numbers of 0.1, 1, and 10 for mass loadings (M) of up to 10 (see also Thevand and Daniel,[5] who studied the effect of compressibility using a similar technique). They observe that the particle-laden mixing layer undergoes the familiar roll-up and pairing similar to the particle-free case, except that the time scales for roll-up and pairing were larger. Note that *ad hoc* diffusion was added to the particle-phase equations in the above work. In the current study, Lagrangian tracking of particles is used, which does not exhibit any numerical diffusion and can capture the formation of very sharp and complicated patterns.

Meiburg *et al.*[6] studied particle settling and the effect of nonuniform seeding of the mixing layer. They showed that when particles are present only in one stream, the particle concentration gradient across the mixing layer leads to a net motion of the vortex in the direction of the seeded stream. They also found that under appreciable gravitational settling of particles, the vortex propagates downward. Wallner and Meiburg[7] performed a study similar to that mentioned above by Wang *et al.*,[4] in which the effect of particles on the pairing process was studied.

[a]Electronic mail: chidu@iet.mavt.ethz.ch
[b]Author to whom correspondence should be addressed. Electronic mail: lakehal@iet.mavt.ethz.ch

TABLE I. Simulation parameters for two-dimensional two-way coupled cases.

No.	St	M	k_{mu}	N_p	R_{rc}	d (mm)
1	0.3	0.1	0.4301	373 000	2	3.67
2	0.3	0.2	0.4206	381 000	4	3.67
3	0.6	0.1	0.4230	379 000	1	5.19
4	0.6	0.2	0.4053	396 000	2	5.19
5a	1.0	0.1	0.4185	305 000	1	6.7
5b	1.0	0.1	0.4185	152 000	2	6.7
5c	1.0	0.1	0.4185	61 000	5	6.7
6	1.0	0.2	0.3962	242 000	2	6.7
7	1.0	0.5	0.3493	275 000	5	6.7
8	2.0	0.1	0.4196	108 000	1	9.48
9	2.0	0.2	0.3952	171 000	1	9.48

In the present study, the Eulerian-Lagrangian method is used to investigate two-way coupling effects in two-dimensional, particle-laden mixing layers for a range of particle Stokes numbers under moderate mass loading. A detailed analysis is performed on the effect of particles on the growth of a two-dimensional mixing layer. The following aspects are addressed: impact of two-way coupling on particle transport, preferential accumulation, and depletion as compared to one-way coupling, effect of particles on the fluid spanwise vorticity, and kinetic energy dissipation, effect of particles on the energy spectrum, on vortex nutation, and on the mechanisms of mixing layer growth embodied in the mean kinetic energy balance, and modal stress evolution.

The presentation is structured as follows. The computational parameters and simulations performed are discussed in the next section. The presentation of results starts with a qualitative description of intricate particle patterns formed and the flow modifications induced by them. Basic particle statistics such as number density and mean vertical velocity are then presented to quantify the impact of two-way coupling on particle transport. The effect of particle loading on the fundamental mode saturation and pairing is presented next, followed by a discussion on the effect of particles in generating small-scale vorticity and on the fluid energy spectra. The mean kinetic energy budget for the fluid flow is presented in detail and the effect of particle loading on the various terms in the budget is discussed.

II. COMPUTATIONAL PARAMETERS AND SIMULATIONS

Two-way coupling results presented in this section were obtained from nine different cases listed in Table I. All the cases were run at a flow Reynolds number of 400, which is defined based on the initial vorticity thickness and the mixing layer velocity difference as length and velocity scales, respectively. For each combination of Stokes number and mass loading, the *most unstable* wave number (k_{mu}) was calculated using linear stability analysis[2] and the streamwise extent of the solution domain was fixed to $4\pi/k_{mu}$ so as to encompass two wavelengths of the fundamental mode. The values of k_{mu} are listed in Table I. All the cases were run with 64 Fourier collocation points in the streamwise direction and 129 Chebyshev collocation points in the vertical direction.

Although the flow is nominally two-dimensional, the simulations with two-way coupling were run in a three-dimensional domain. A spanwise domain size was chosen such that there were between 200 000 and 400 000 particles in the domain. This number was chosen so that there were enough particles in the domain to obtain reasonable averages. This methodology was used successfully in a previous study,[8] in which it was shown that the results are independent of the chosen spanwise extent. The number of nodes in the spanwise direction was chosen as required by the interpolation stencil for calculating the fluid velocity at particle positions (four nodes for the fourth-order method).

The flow was initialized using a hyperbolic-tangent streamwise velocity profile perturbed using the eigenfunctions obtained from the linear stability analysis. The amplitudes of the fundamental and subharmonic perturbations were set to $\epsilon_f = 10^{-2}$ and $\epsilon_s = 10^{-4}$ (same as for one-way coupling). The particle Stokes numbers, mass loadings, and diameters for the simulations presented are given in Table I. The particle-to-fluid density ratio was set to 1000 for all the cases; therefore the volume fractions can be obtained by dividing the mass loadings by the density ratio. Note that the maximum volume fraction 5×10^{-4} occurs for case 7.

A. Effect of number of particles

In point-particle methods, it is not desirable (for reasons of computational time) to account for all the particles in the domain for a given mass loading; instead, only a fraction of the total number of particles is tracked and the two-way coupling force acting on each particle is appropriately weighted to obtain the total force. A systematic sensitivity study with different numbers of particles has been performed to validate the results. The values for the ratio of the number of real to computational particles (R_{rc}) used here are typically quite small compared to those of many three-dimensional simulations reported, in which this problem is more acute.[9]

Evidently, as long as there is a significant number of particles in the domain, a reasonable factor should not result in significantly different results. As reported in the above table, for the two-dimensional mixing layer calculations, this factor was usually around 2, and not higher than 5 for the high-mass-loading case. Tests were performed to verify that the assumed ratios do not change the results appreciably, and in a systematic way (cases 5a, 5b, and 5c). The effect of the amplitude of the initial perturbation was also tested. Cases 5b and 5c were first computed with higher values of the initial perturbation amplitudes: $\epsilon_f = 0.1$ and $\epsilon_s = 0.005$. The evolution of the fundamental and subharmonic energies for the two cases are compared in Fig. 1(a). The two computations give very similar, almost overlapping, results for $R_{rc} = 2$ and 5.

For the lower amplitudes used in all the simulations reported, the growth of the subharmonic mode was affected by changing R_{rc} to some extent [Fig. 1(b)]. Because the initial amplitude of the subharmonic is very small, there is a non-negligible influence in the long-time evolution of the subhar-

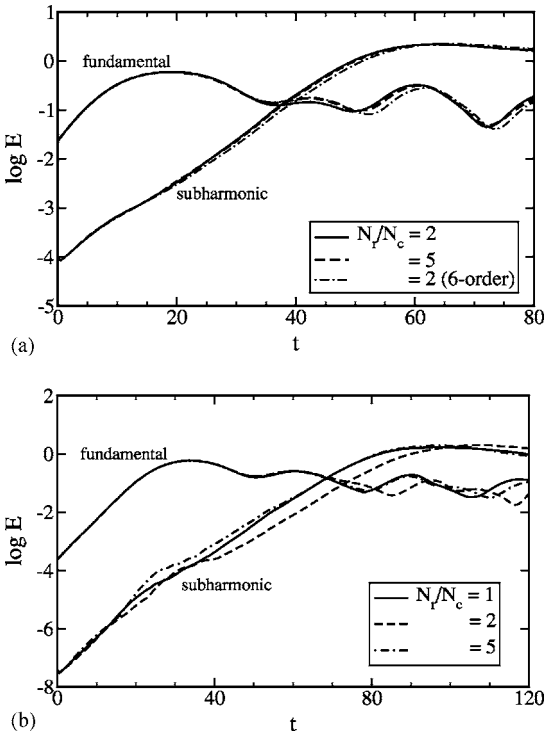

FIG. 1. Evolution of the fundamental and subharmonic energies for different R_{rc} and different initial perturbation amplitudes. (a) Higher amplitudes; (b) normal amplitudes.

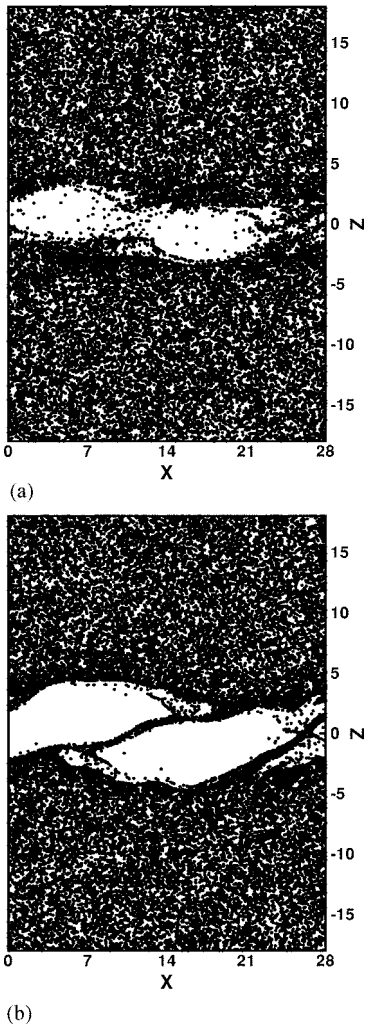

FIG. 2. Particle patterns at $t=72$ for mass loading of 0.2. (a) St=0.3; (b) St=0.6.

monic mode. This influence was found not be of a deterministic nature and does not show any particular trend. Runs were also made in which the initial random particle distribution was different (random sequences with different seed values). The results showed similar small variations, but with deviations showing no systematic influence on the evolution of the mixing layer.

B. Effect of velocity interpolation method

Two important numerical aspects in the Lagrangian tracking of particles under two-way coupling are the interpolation method to calculate the fluid velocity at the particle position, and the distribution of the particle force onto the fluid grid points. In this study, a fourth-order Lagrangian polynomial interpolation is used. In a previous study[10] by the authors, it was shown by comparison to a sixth-order method, that for this class of problems a fourth-order method is sufficient. In Fig. 1(a) the evolution of the fundamental and subharmonic energies computed with a sixth-order scheme is also presented. No significant differences can be observed over the whole integration time duration.

In the same study,[10] the effect of two different force distribution methods was also tested. In one method, the particle force is distributed to the eight corners of the cell in which the particle is located; in the second method (proposed by Sundaram and Collins[11]), the force is distributed back to the interpolation stencil used to calculate the fluid velocity at the particle position. No distinguishable differences were observed. In the present study the latter method has been employed.

III. PARTICLE ACCUMULATION PATTERNS AND EFFECT ON SPANWISE VORTICITY

Preferential accumulation of particles depends not only on the inertia of the particles and the time-scale and intensity of flow structures, but also on their *lifetime*. In the present case, the Kelvin-Helmholtz (KH) vortices saturate at $t=32$ and nutate undisturbed until $t \approx 70$. In this time duration, particles get centrifuged out of the core. The *lifetime* of the KH vortices is meant to denote the time duration $t \approx 20-70$. This duration can be adjusted by choosing a higher or lower initial subharmonic energy such that pairing occurs earlier or later. Due to the sustained action of the KH vortices, even particles with small Stokes numbers migrate from the core of the vortices to the edges and to the braid region in between the vortices. The concentration of particles at the periphery of the vortices can be quite high, especially for higher-Stokes-number particles. This has been shown in Part I under the assumption of one-way coupling.

Particle patterns for Stokes numbers 0.3 and 0.6 at a mass loading of 0.2 are shown in Figs. 2 and 3, at times $t=72$ and 96, respectively. Comparison with the corresponding patterns under one-way coupling (Fig. 13 in Part I) al-

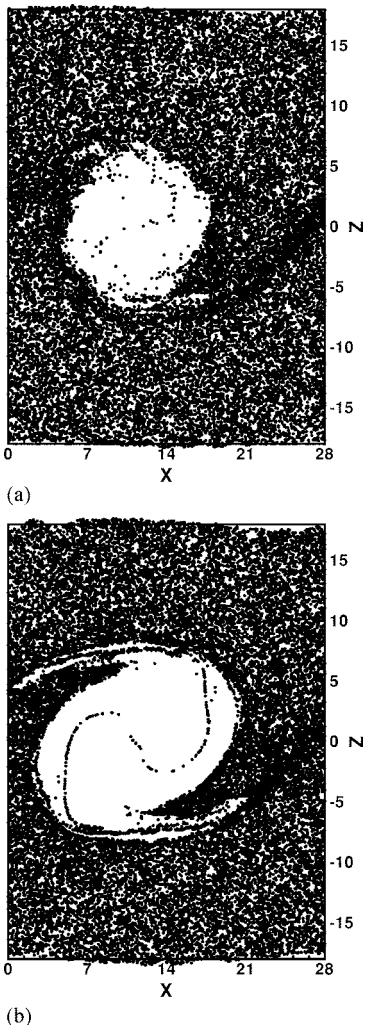

FIG. 3. Particle patterns at $t=96$ for mass loading of 0.2. (a) St=0.3; (b) St=0.6.

ready reveals a small distortion of the spanwise vortices. At $t=96$, the shape of the evacuated region is significantly different and the patterns no longer have clear and distinct boundaries.

Particle pattern sequences for mass loadings of 0.2 and 0.5 for Stokes numbers of 1 and 2 are presented in Figs. 4 and 5. At these mass loadings, particles have a strong impact on the flow, especially in the peripheral regions of the vortices. The effect is dramatic for St=1 and $M=0.5$, where the particle patterns are unlike those at lower mass loadings. It appears that the ability of the KH vortices to centrifuge particles away from their core has been reduced significantly.

Sharp undulating patterns with an intricate structure are formed at the periphery of the vortices. This can be seen in Fig. 6, which shows a magnification of the braid region of Fig. 4(a) and the top right corner of one of the vortices of Fig. 5(b). From linear stability analysis it is known[2] that no new flow instability is introduced by the addition of uniformly distributed particles at low mass loadings. The mechanism for the formation of these patterns is primarily the local drag interaction between the accumulated particles and the flow. Due to high concentration of particles in the periphery, small scale velocity is generated, which locally advects the particles to eventually form the patterns. In other words, it is induced purely by particle transport by the flow and the fluid-particle interaction. Even if the small scales are not dynamically significant due to their low energy content in these two-dimensional flows, such patterns could be important for allied processes involving phase change (for example, evaporation of droplets) or combustion.

In the study by Wang *et al.*,[4] who analyzed the impact of particles on the saturation and pairing times, particle accumulation patterns were not presented. In addition, it is possible that such patterns would not appear in the Eulerian-Eulerian simulation approach used by them due to numerical diffusion. Therefore, the formation of particle patterns is one of the important findings of the present work; especially because various numerical consistency checks have been performed with respect to number of particles, interpolation accuracy, grid refinement, etc.

Effect on spanwise vorticity

The rupture of the KH vortices can be observed clearly in Fig. 7, which shows spanwise vorticity contours at $t=72$, for mass loadings of 0.1, 0.2, and 0.5. Even for a mass loading of 0.1, local positive and negative vorticity is generated. At the periphery of the vortices strong gradients of vorticity are evident. For a mass loading of 0.2, the vortex structures are affected and the pairing is visibly delayed. For mass loading of 0.5, it is difficult to describe the flow in familiar terms: the vortex is broken up into chunks and significant small-scale vorticity has been generated. Strong effects at global mass loadings as small as 0.1–0.5 are observed for this two-dimensional flow.

At $t=96$ (Fig. 8) especially for a mass loading of 0.5, sheets of positive and negative vorticity are present [see Fig. 13(a)]. As mentioned by Druzhinin,[3] the generation of sheets of increased particle concentration results in the generation of vortex sheets which contribute to energy cascade towards smaller scales and cause a higher dissipation rate in particle-laden flows as shown later. The shading legend in Fig. 8(d) shows that the spanwise vorticity range is approximately three times (−1.2 to 1.9) the range in a particle-free mixing layer (0 to 1).

IV. FUNDAMENTAL MODE SATURATION AND PAIRING

Two quantities characterizing the overall impact of particles in a temporally evolving mixing layer are the time to *saturation* of the fundamental mode and the *initiation* of pairing. Results from linear stability analysis suggest that particles with small and large Stokes numbers leave the instability growth rates only slightly lower.[2] On the other hand, intermediate Stokes number particles not only significantly reduce the growth rates, but also modify the most unstable wave number. A similar behavior can be expected with regard to the later period of growth and saturation of the fundamental mode. As shown in Fig. 9(a), the time to saturation increases due to the addition of particles in all cases, but the maximum increase happens for intermediate Stokes numbers

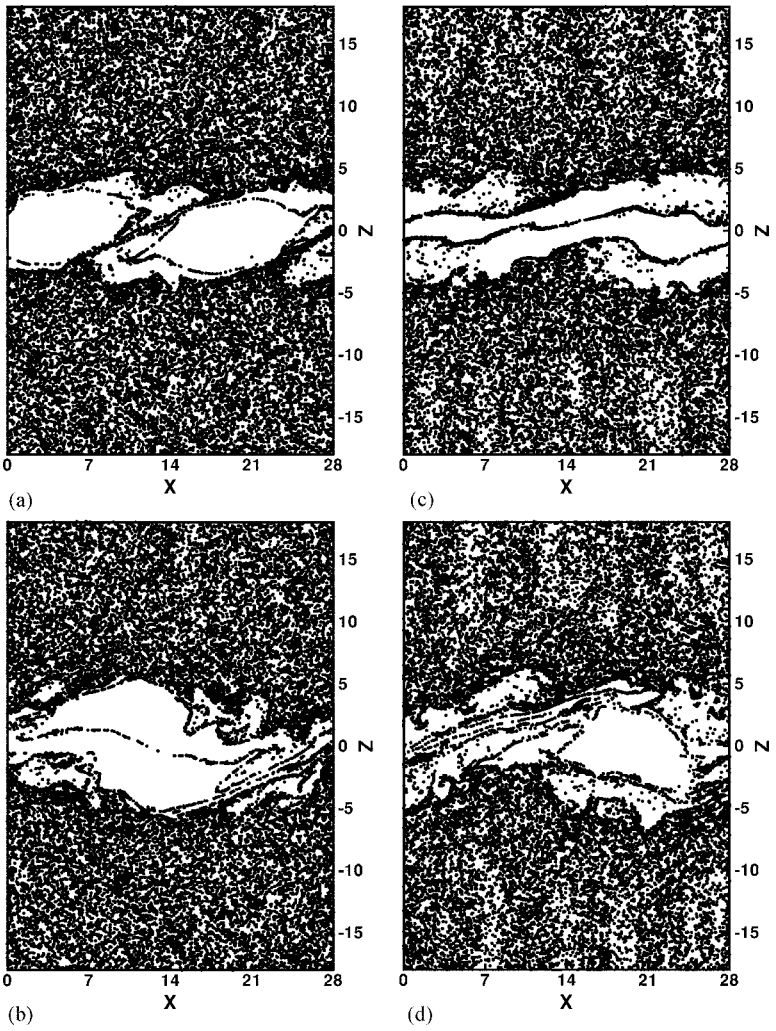

FIG. 4. Particle patterns for St=1. (a) $M=0.2$, $t=72$; (b) $M=0.2$, $t=96$; (c) $M=0.5$, $t=72$; (d) $M=0.5$, $t=96$.

of the order of unity. The dotted lines in Fig. 9 represent the saturation and initiation times for the particle-free mixing layer. For a mass loading of 0.5, the increase in the saturation time is large (more than ten nondimensional units). This increase affects the initiation of pairing, which can happen earlier or later than for the particle-free case depending on the time of saturation, and the effect of particles on the growth of the subharmonic mode. The time of initiation of pairing is defined here as the time when the energies of the fundamental and subharmonic modes intersect.

Figure 9(b) shows that for a mass loading of 0.1 the initiation of pairing is accelerated for the smaller Stokes numbers and delayed for St=2 and higher. For a mass loading of 0.2 the pairing is delayed for a larger range of Stokes numbers. Note the peculiar behavior of St=1 particles: The time to initiation of pairing is smaller than the particle-free case for mass loadings of 0.1 and 0.5, but is significantly larger for mass loading of 0.2. The reason for this peculiarity is evident in Fig. 10, which shows the evolution of the fundamental and subharmonic energies for St=1 and different mass loadings. The growth rate of the subharmonic mode is reduced by St=1 particles monotonically with increasing mass loading. Therefore, if the fundamental mode evolution remains unchanged, then pairing should get delayed monotonically, too. However, it is seen that the energy in the fundamental mode after saturation is also reduced significantly with increasing particle loading. Therefore, the subharmonic energy needed for the two energies to intersect is also lower. Thus, the initiation of pairing does not have a simple functional dependence on mass loading. However, the saturation of the subharmonic mode (which denotes the end of pairing) shows a monotonic delay with mass loading, along with a reduction in the energy levels at saturation.

In the study by Wang *et al.*[4] the fundamental saturation for St=1 particles at different mass loadings were found to be almost the same. This is different from that obtained here and needs further explanation. In both simulations, the streamwise domain size is adjusted to take into account the decrease in the most unstable wave number for a particular mass loading and Stokes number. Since we know that the growth rate is significantly affected by particles as mass loading is increased, it is natural to expect a longer time for fundamental saturation, as found in the present study. However, a closer look at the study[4] reveals that in their simulations, the subharmonic and fundamental energies are of similar magnitude during fundamental saturation. Thus, the fundamental mode saturates independent of particle loading because the subharmonic has a higher growth rate and takes up more energy from the mean flow. In the present study, the subharmonic energy is four orders of magnitude lower at

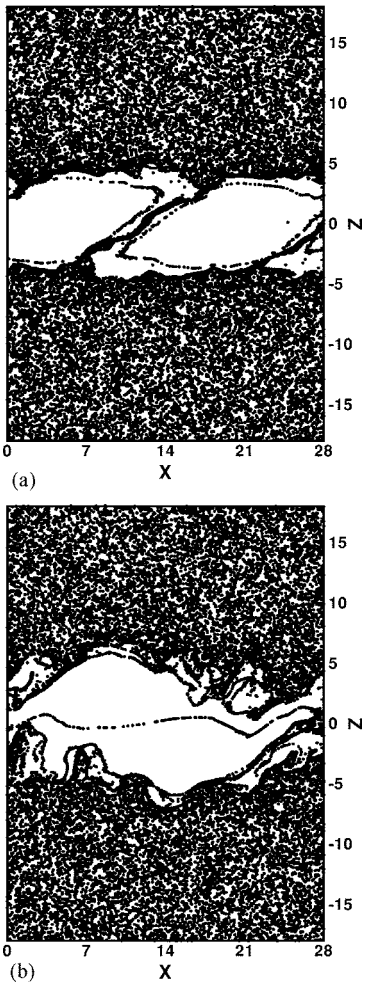

FIG. 5. Particle patterns for St=2 and mass loading of 0.2. (a) $t=72$; (b) $t=96$.

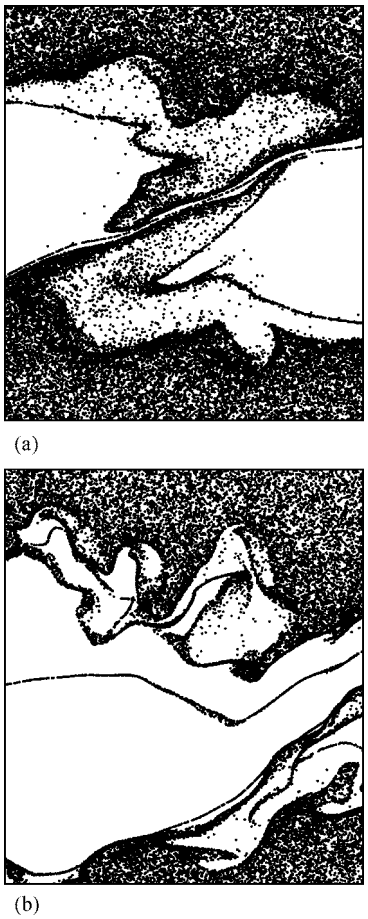

FIG. 6. Magnified view of particle patterns for mass loading of 0.2. (a) Zoom of Fig. 4(a); (b) zoom of Fig. 5(b).

fundamental saturation, and it does not interfere with fundamental mode growth and saturation.

V. PARTICLE STATISTICS

The fact that the centrifuging effect of the Kelvin-Helmholtz vortices is lower under two-way coupling is clearly seen in the number density plots for St=1 at different mass loadings (Fig. 11). As in Part I, local Eulerian quantities such as number density (n) and particle velocity (u_{pi}) are calculated by averaging in a volume around the computational node, which are then averaged over the horizontal plane to yield average quantities such as $\langle n \rangle$ and $\langle w_p \rangle$ presented here. Although the initial lower rate of growth of the instability modes is a cause for this observation, the differences in particle concentration as compared to one-way coupling remain significant through out the duration of the simulation. A complete evacuation of the central core of the mixing layer never occurs.

The same is true for the particle-phase mean vertical velocity. In the case of two-way coupling the mean vertical velocities are much smaller than the one-way coupling case. The difference is most visible at times 48 and 96 [Figs. 12(b) and 12(d)], where, in the one-way coupled case, the centrifuging velocity is large and well developed. At $t=96$ for $M=0.2$, and 0.5, the velocity profiles imply re-entrainment into the mixing layer.

From the above particle statistics, one can conclude that although intricate patterns of particle segregation are formed due to two-way coupling, the overall particle concentration due to the large-scale KH vortices is significantly smaller resulting in a more even distribution of particles.

VI. GENERATION OF SMALL SCALES

As already mentioned, the highly localized accumulation of particles results in the generation of small scales, as evident in Figs. 7 and 8. In a particle-free mixing layer, the spanwise vorticity is positive everywhere except in the free-stream, where it is zero. With the addition of particles, local negative vorticity regions are created with magnitudes of the order of the mean spanwise vorticity. For example, if there is a very high concentration of particles in a small region, the localized interaction force can cause a lag in the velocity to create a negative gradient. The magnitude of this effect is shown in Fig. 13(a), where the evolution of the maximum and minimum of the spanwise vorticity is presented. The positive vorticity is enhanced 2–3 times and the maximum negative vorticity has almost the same magnitude. This

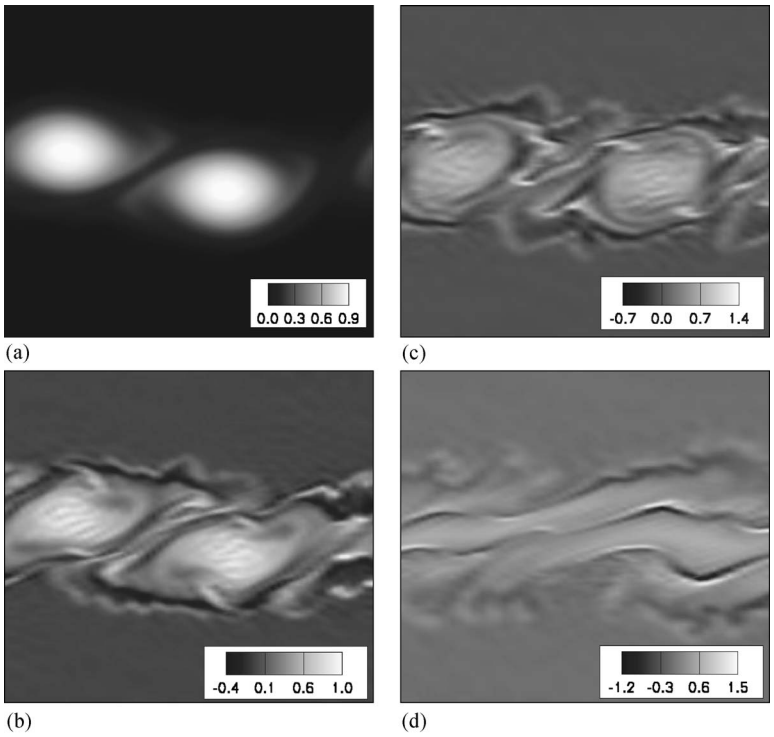

FIG. 7. Spanwise vorticity contours at $t=72$ for St=1 particles at different mass loadings. (a) No particles; (b) $M=0.1$; (c) $M=0.2$; (d) $M=0.5$.

shows that small-scale vorticity, or simply small scales, are produced.

As a direct consequence of the production of small scales, we see an increase in the viscous dissipation rate of the modal kinetic energy [Fig. 13(b); Eq. (9) in Part I], which is around 2–3 times larger for the cases with mass loading of 0.2, and up to 7 times larger for mass loading of 0.5.

Effect on the energy spectrum

Simulations of particle-laden isotropic turbulence (both decaying and forced) have shown that particles increase the energy in the small scales.[9,12] A similar situation is observed here for two-dimensional mixing layers undergoing pairing; Fig. 14 shows the power spectra of the streamwise velocity

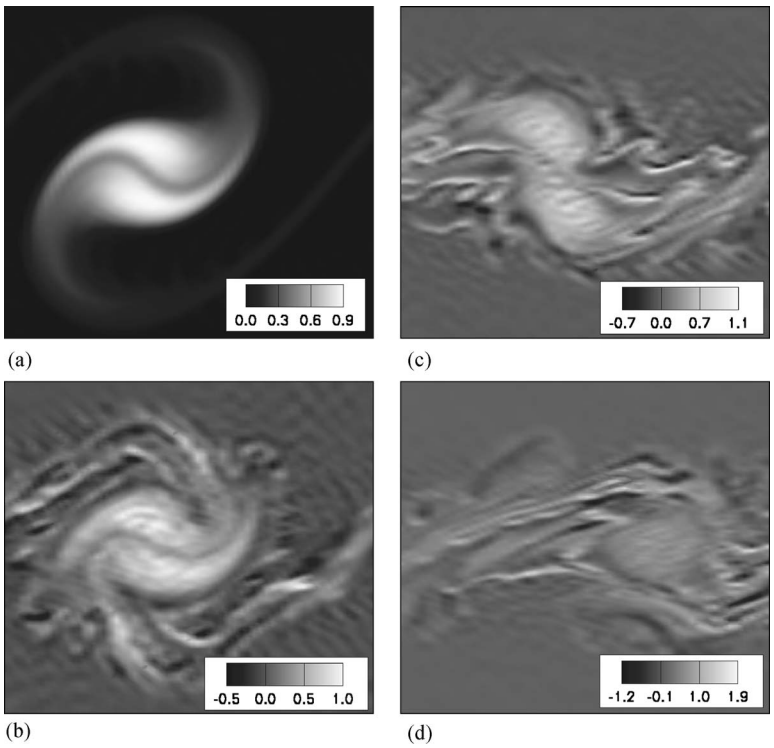

FIG. 8. Spanwise vorticity contours at $t=96$ for St=1 particles at different mass loadings. (a) No particles; (b) $M=0.1$; (c) $M=0.2$; (d) $M=0.5$.

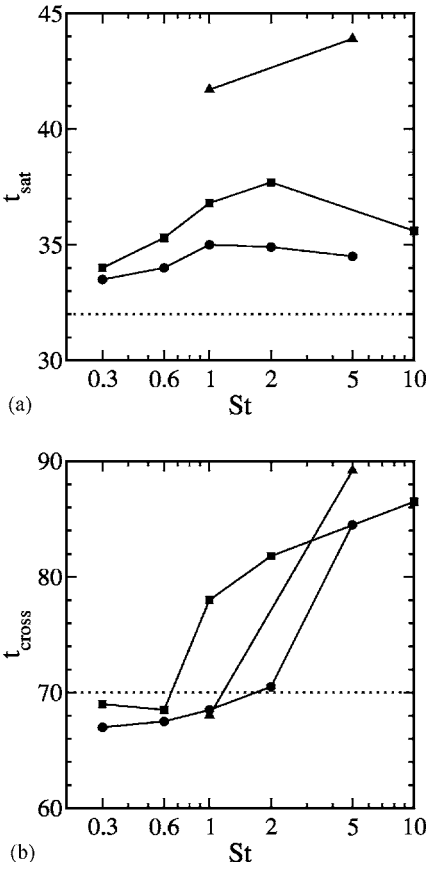

FIG. 9. Variation of (a) fundamental mode saturation time, and (b) initiation of pairing time, with particle Stokes number and mass loading. Symbols: (○○○) $M=0.1$; (□□□) $M=0.2$; (△△△) $M=0.5$.

at $t=96$ for all the cases simulated. Although in the case of the two-dimensional mixing layer, the energy in the small scales (smaller than the fundamental mode and its first harmonic) is very small to be dynamically significant, the increase in the energy at these scales is noteworthy. The increase is directly proportional to both the Stokes number and the mass loading for the range of parameters considered.

Since an increase in the energy in the small scales is observed, one can question the adequacy of the current resolution of the flow. Case 6 (St=1 and mass loading 0.2) was recalculated with 128 Fourier collocation points in the streamwise direction to check if the simulation was adequately resolved. The comparison of the evolution of the fundamental and subharmonic energies is presented in Fig. 15(a). It shows that although some differences exist, the overall evolution has not changed appreciably. Figure 15(b) compares the power spectra obtained using the two resolutions at $t=72$. The energy spectra from the lower resolution case match the higher resolution case.

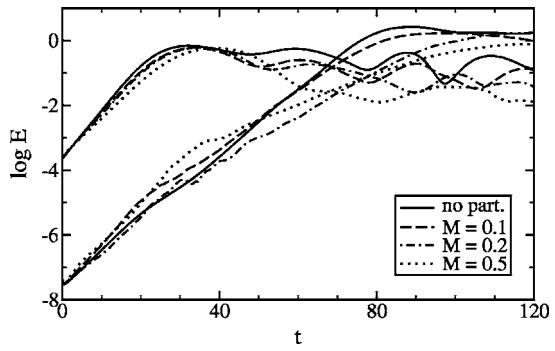

FIG. 10. Evolution of the fundamental and subharmonic energies for St=1 particles at different mass loadings.

VII. EVOLUTION OF AVERAGE MODAL STRESS

The various stages of evolution of a mixing layer can be well understood by the evolution of the averaged modal stress. A positive value implies transfer of energy from the mean to the modes, and vice versa. Figure 16 presents the evolution of the averaged modal stress for the particle-free case and for particle Stokes numbers of 0.3, 0.6, and 1.0 at mass loading of 0.1. It can be seen that in the particle-laden cases, the initial backward transfer of energy from the modes to the mean (approximately $t=32-60$) is larger. The subsequent oscillation present in the particle-free case is also suppressed; this implies that the vortex nutation process is significantly affected. Overall the number of zero-crossings of the modal stress $-\langle u'w'\rangle_{\text{norm}}$ is reduced (eight crossings for the particle-free case, compared to 3–4 for the particle-laden cases). The dynamic exchange of energy between the mean and modal flow components is significantly slowed down by the presence of particles, which seem to make the flow more sluggish.

VIII. MEAN KINETIC ENERGY BALANCE

The effect of particles on the mean kinetic energy budget of the fluid flow is presented in this section. The balance of the mean kinetic energy $\langle k\rangle=\frac{1}{2}\langle u_i\rangle\langle u_i\rangle$ is given as follows:

$$\underbrace{\frac{\partial\langle k\rangle}{\partial t}}_{\text{(I)}}=\frac{1}{\mathrm{Re}}\frac{\partial^2\langle k\rangle}{\partial z^2}-\frac{1}{\mathrm{Re}}\left(\frac{\partial\langle u\rangle}{\partial z}\right)^2-\underbrace{\frac{\partial}{\partial z}(\langle u\rangle\langle u'w'\rangle)}_{\text{modal transp. (II)}}+\underbrace{\langle u'w'\rangle\frac{\partial\langle u\rangle}{\partial z}}_{\text{exchange (III)}}+\underbrace{\langle u\rangle\langle f_{x,CD}\rangle}_{\text{force term (IV)}}, \tag{1}$$

where the first two and the fourth terms in the right-hand side are the viscous diffusion, viscous dissipation, and the energy exchange between the mean and the modes (modes include all finite length scales in the flow; however, most of the energy is accounted for by the fundamental and the subharmonic modes). The third term is the convective transport of mean kinetic energy by the modes and the last term is the energy exchange between the particles and the mean flow.

The cases with low mass loading (Cases 1, 3, and 5) were selected instead of the high mass loading cases so that the effect of two-way coupling can be studied as a point of departure from the particle-free case. One of the effects of particles is to delay the flow evolution such that different cases are at different stages of evolution at a given time. Therefore, a direct comparison between the structure of the transport mechanisms for different flows has to take this aspect into account. For the higher mass loadings, the delay is significant (Fig. 9) making comparisons difficult. Two times

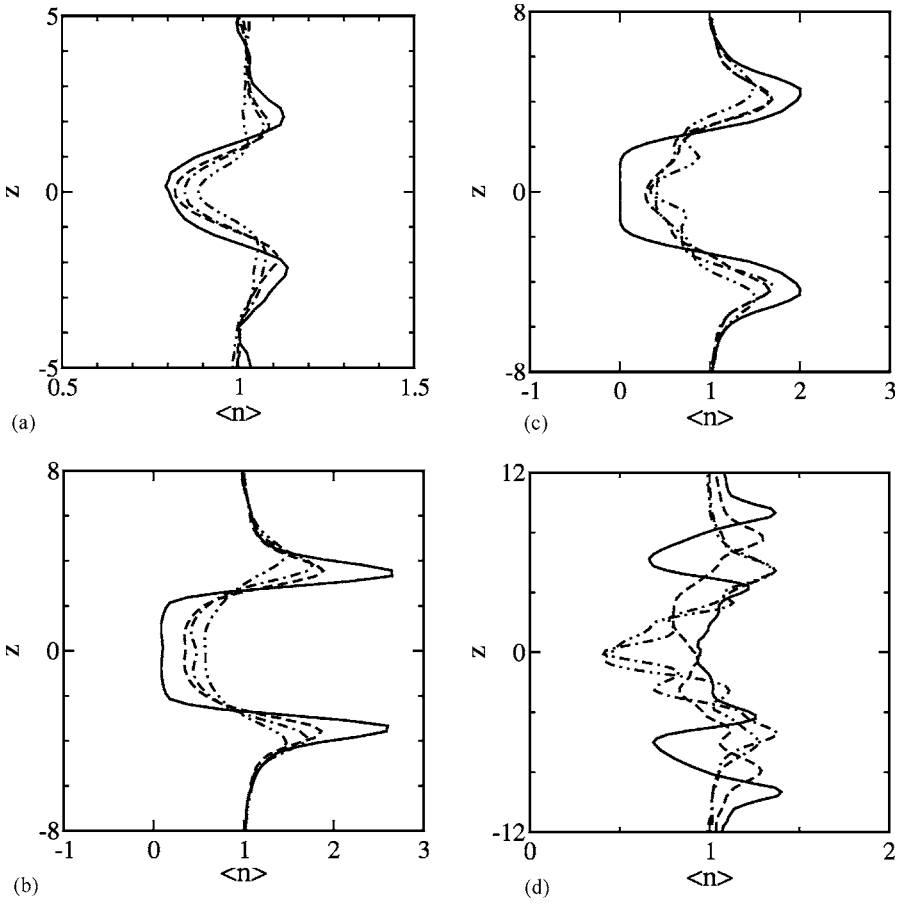

FIG. 11. Particle number density profiles for St=1 at different mass loadings. Legend: (—) one-way coupling; (——) $M=0.1$; (–·–) $M=0.2$; (–···–) $M=0.5$. (a) $t=24$; (b) $t=48$; (c) $t=72$; (d) $t=96$.

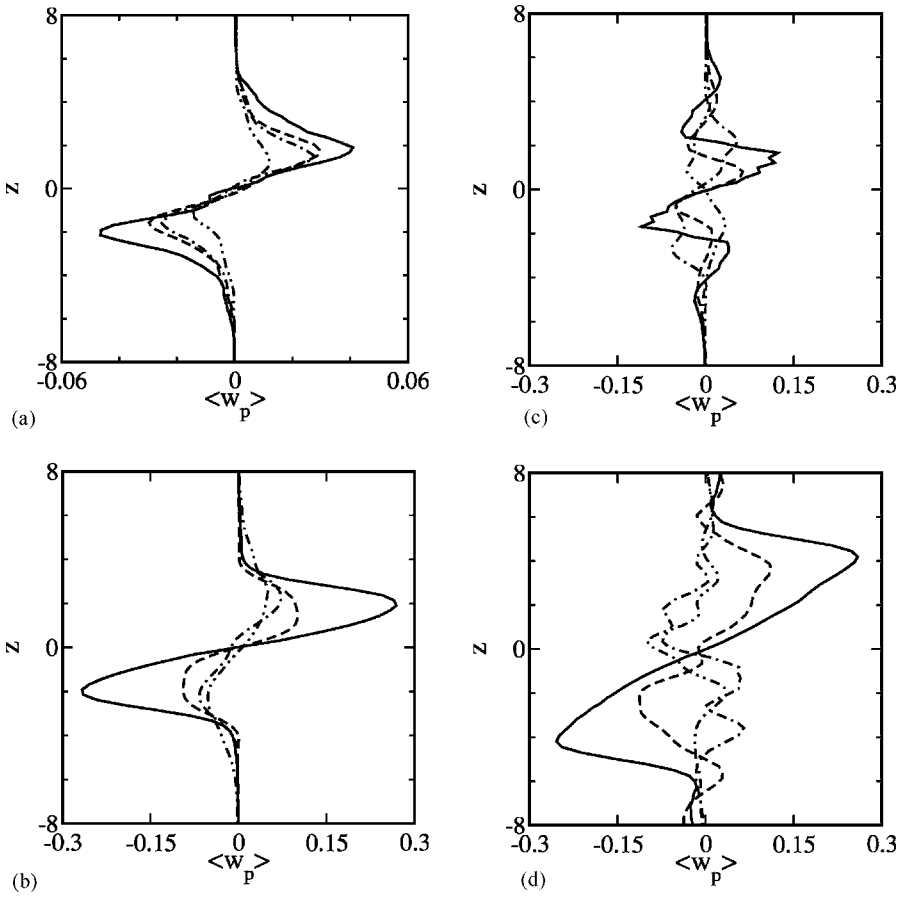

FIG. 12. Mean particle-phase vertical velocity profiles for St=1. Legend: (—) one-way coupling; (——) $M=0.1$; (–·–) $M=0.2$; (–···–) $M=0.5$. (a) $t=24$; (b) $t=48$; (c) $t=72$; (d) $t=96$.

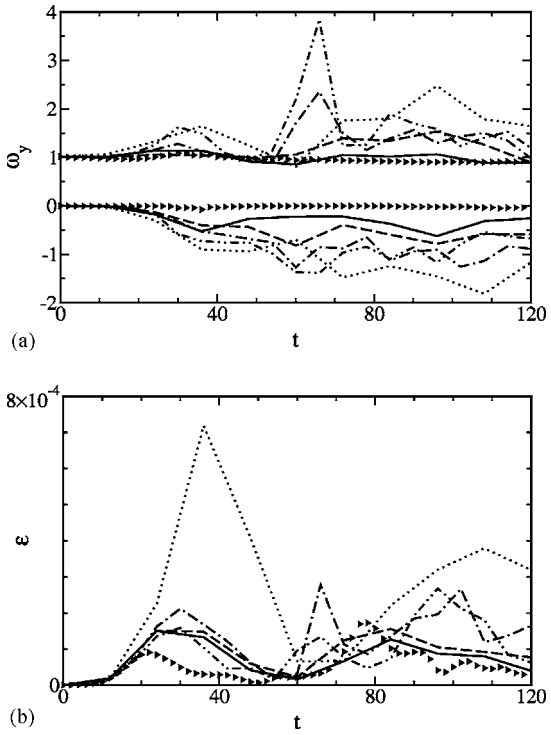

FIG. 13. Effect of particles on (a) maximum and minimum spanwise vorticity and (b) modal dissipation rate. Legend: (▷▷▷) no particles. Mass loading of 0.2, (—) St=0.3; (——) St=0.6 (–·–) St=1; (–··–) St=2. Mass loading of 0.5, (·····) St=1.

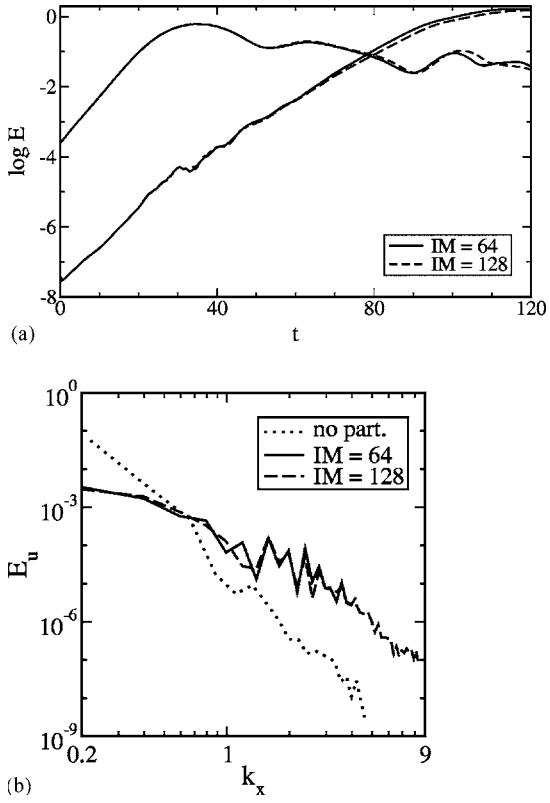

FIG. 15. (a) Evolution of the fundamental and subharmonic energies for different streamwise mesh resolutions. (b) Energy spectra at different streamwise mesh resolutions at $t=72$.

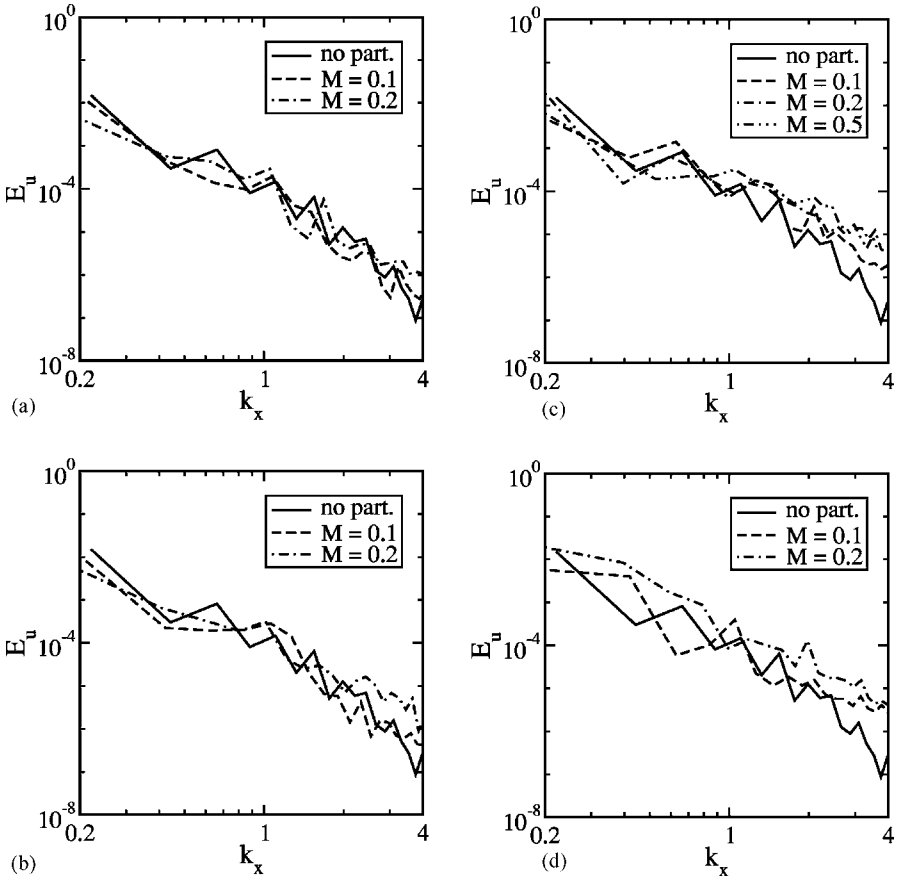

FIG. 14. Power spectrum of streamwise velocity for different Stokes numbers at $t=96$. (a) St=0.3; (b) St =0.6; (c) St=1; (d) St=2.

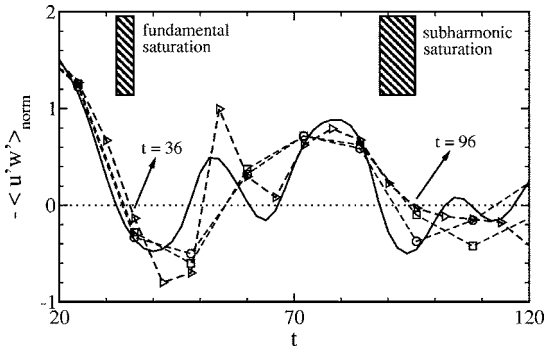

FIG. 16. Evolution of the averaged modal stress for mass loading of 0.1. Legend: (—) no particles; (○○○) St=0.3; (□□□) St=0.6; (▷▷▷) St=1.

are chosen for the kinetic energy budgets: a time immediately after fundamental mode saturation ($t=36$) and after subharmonic mode saturation ($t=96$). The time windows for the two situations are also shown in the Fig. 16. Note that even within the windows, the flows are under different evolution stages and this issue complicates the direct comparison with the case with one-way coupling.

The mean kinetic energy balance at $t=36$ is presented in Figs. 17(a)–17(d). The profiles were smoothed using a *running average* option in the plotting package using an eight-point stencil. The viscous terms are negligible and are not presented. In their experiments, Kiger and Lasheras[13] found that in the early stages of the flow evolution, most of the kinetic energy exchange between the phases occurs at the edges of the mixing layer. This is clearly observed in Fig. 17(d), which shows the average kinetic energy lost from the mean flow due to particle interaction. Part of this energy is transferred to the particles and a part is dissipated. The mean kinetic energy exchange between the phases is very small at the center of the layer. The exchange increases with Stokes number, and this is partly due to the increased accumulation of particles and partly due to the higher magnitude of the drag force.

The modal transport and energy exchange terms [shown in Figs. 17(b) and 17(c)] show a monotonic variation with Stokes number. However, this is only indirectly attributable to two-way coupling, which causes a relative lag in the evolution of the mixing layers as shown in Fig. 16. For example, for St=1 the modal stress has just changed signs, whereas for the particle-free case it has almost reached a local minimum. The net effect of the three terms is shown in Fig. 17(a), which represents the rate of change of the mean kinetic energy. Note that the time derivative is not calculated directly, but is only estimated by summing up all the spatial terms in Eq. (1). Accounting for the delay in the flow evolution, the main effect of particle two-way coupling is near the edge of the mixing layer where the drag force term induces a change in the sign of the time derivative term.

At $t=96$ significant lag exists in the evolution of the flow in the different cases. The subharmonic mode has just saturated for St=1 and 0.6, whereas it has passed the local minimum for the particle-free case. Keeping this in mind, we look at the mean kinetic energy balance terms shown in Fig.

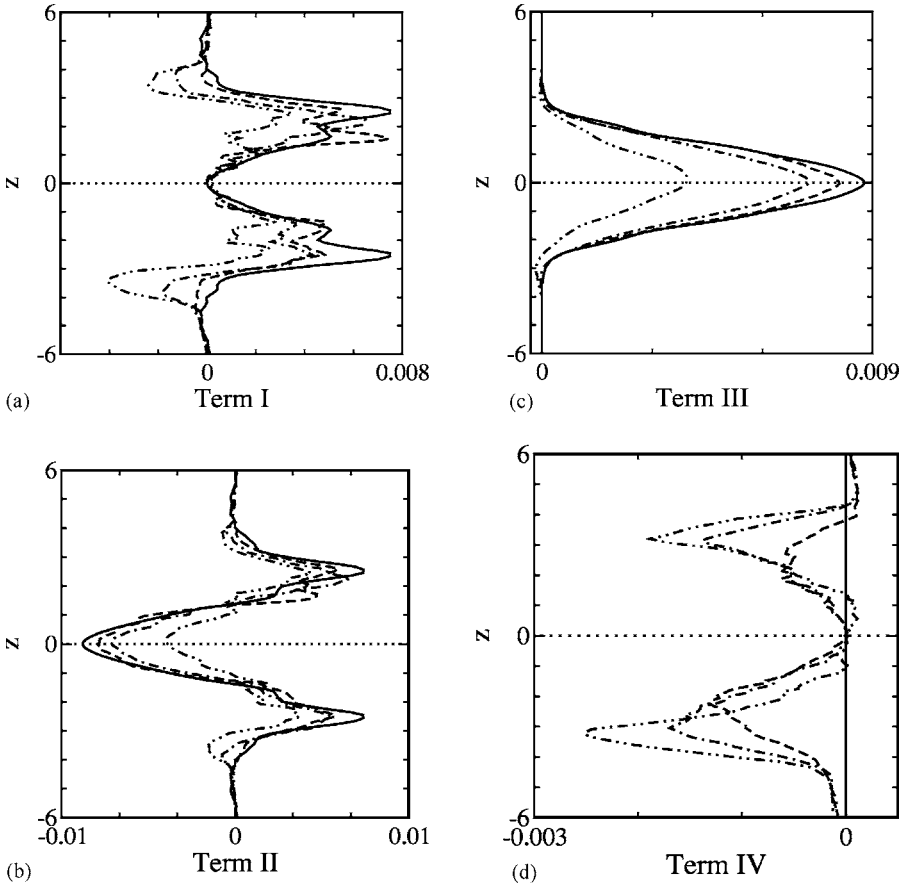

FIG. 17. The mean kinetic energy balance $t=36$ under two-way coupling. Legend: (—) no particles; (——) St =0.3; (–··–) St=0.6; (–···–) St=1. (a) Time derivative term; (b) modal transport term; (c) energy exchange term; (d) drag force term.

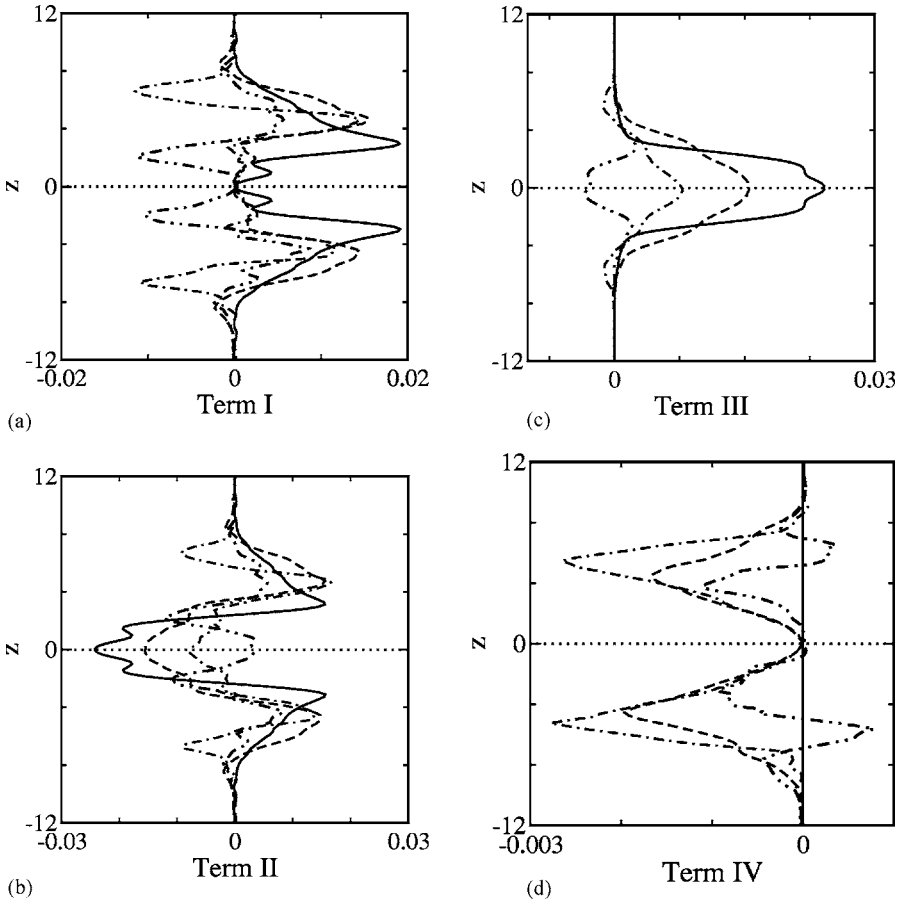

FIG. 18. The mean kinetic energy balance $t=96$ under two-way coupling. Legend: see Fig. 17. (a) Time derivative term; (b) modal transport term; (c) energy exchange term; (d) drag force term.

18. Two important observations can be made: first, the energy exchange term and the modal transport term have increased in magnitude as compared to the drag force term, which remains of the same magnitude as compared to $t=36$. This is due to the fact that the mean value of the particle Reynolds number reaches a constant value after an initial build up (see Fig. 11 in Part I). This points to a decrease in importance of the drag interaction in the overall fluid mean kinetic energy balance with time. Second, two-way coupling has increased the lateral spread of the mixing layer, as shown by higher activity near the edges of the layer [Fig. 18(b)]. The main kinetic energy transfer between the particle and the fluid phases is still restricted to the edges of the mixing layer.

Also noteworthy is the fact that at both time instants presented, particles on an average receive energy from the mean flow, which results in a more monotonic increase in the momentum thickness of the layer; this is in contrast to a particle-free mixing layer where increase in momentum thickness is sporadic, related mainly to fundamental mode saturation and then pairing.

IX. CONCLUSION

Two-way coupled simulations of two-dimensional particle-laden mixing layers were performed for particles with various Stokes numbers for mass loadings between 0.1 to 0.5. It was shown that the accumulation of particles in the periphery of the vortices results in the formation of sharp undulating patterns and rupture and break-up of the vortices for the higher Stokes numbers. For higher mass loadings, the vortex structure was completely destroyed. The accumulation of particles at the periphery of the Kelvin-Helmholtz vortices was significantly reduced due to two-way coupling. Overall, a more uniform distribution of particles was observed, in spite of local small-scale pattern formation. The magnitude of particle-phase mean vertical velocity was much smaller.

In a global sense, particles delay the development of the mixing layer in terms of the saturation of the fundamental and subharmonic modes. The delay was shown to be the highest for intermediate Stokes numbers. For a mass loading of 0.5 the delay in fundamental mode saturation was as high as ten nondimensional time units. The energy in the fundamental and the subharmonic modes, after their respective saturation, was significantly reduced with increased particle mass loading.

Significant generation of small scale vorticity was observed for higher mass loadings resulting in higher energy in the small scales. This is due to the local drag-force interaction between the accumulated particles and the underlying fluid flow. The accumulation of energy in the small scales was shown to increase with Stokes number and mass loading. The average modal stress evolution showed that the presence of particles suppresses the dynamics of energy exchange between the mean and modal flow components, which results in a more monotonic growth in the mixing layer momentum thickness.

The mean kinetic energy balance for the fluid phase showed that most of the kinetic energy exchange between the particle and fluid phases takes place at the edges of the mixing layer. As the mixing layer evolves, the kinetic energy exchange with the particle phase was shown to decrease in importance compared to the other terms in the mean kinetic energy balance; namely, the energy exchange between the mean and the modal fields and the modal transport term.

This study has focused primarily on the effect of particles on the flow evolution, except the discussion on particle concentration and mean vertical velocity profiles. The impact of two-way coupling on the particle transport is yet to be analyzed in detail, as in Part I.

ACKNOWLEDGMENTS

The authors would like to thank Professor Yadigaroglu for his support and guidance. C.N. would like to thank the Leonhard Euler Center of the European Research Community on Flow Turbulence and Combustion (ERCOFTAC) for funding this research.

[1] A. A. Dimas and K. T. Kiger, "Linear instability of a particle-laden mixing layer with a dynamic dispersed phase," Phys. Fluids **10**, 2539 (1998).
[2] C. Narayanan and D. Lakehal, "Temporal instabilities of a mixing layer with uniform and nonuniform particle loadings," Phys. Fluids **14**, 3775 (2002).
[3] O. A. Druzhinin, "On the two-way interaction in two-dimensional particle-laden flows: the accumulation of particles and flow modification," J. Fluid Mech. **297**, 49 (1995).
[4] L.-P. Wang, X.-L. Tong, and J. DeSpirito, "Two-way coupled particle-laden mixing layer part 2: Nonlinear evolution," in Third International Conference on Multiphase Flow, Lyon, France, 1998.
[5] N. Thevand and E. Daniel, "Nonlinear development of particle-laden mixing layers at low mach numbers," AIAA J. **42**, 2082 (2004).
[6] E. Meiburg, E. Wallner, A. A. Riaz, C. Haertel, and F. Necker, "Vorticity dynamics of dilute two-way-coupled particle-laden mixing layers," J. Fluid Mech. **421**, 185 (2000).
[7] E. Wallner and E. Meiburg, "Vortex pairing in two-way coupled, particle laden mixing layers," Int. J. Multiphase Flow **28**, 325 (2002).
[8] D. Lakehal and C. Narayanan, "Numerical analysis of the continuum formulation for the initial evolution of mixing layers with particles," Int. J. Multiphase Flow **29**, 927 (2003).
[9] S. Elghobashi and G. C. Truesdell, "On the two-way interaction between homogeneous turbulence and dispersed solid particles. I. Turbulence modification," Phys. Fluids A **5**, 1790 (1993).
[10] C. Narayanan, D. Lakehal, and G. Yadigaroglu, "Linear stability analysis of particle-laden mixing layers using lagrangian particle tracking," Powder Technol. **125**, 122 (2002).
[11] S. Sundaram and L. R. Collins, "A numerical study of the modulation of isotropic turbulence by suspended particles," J. Fluid Mech. **379**, 105 (1999).
[12] A. Ferrante and S. Elghobashi, "On the physical mechanisms of two-way coupling in particle-laden isotropic turbulence," Phys. Fluids **15**, 315 (2003).
[13] K. T. Kiger and J. C. Lasheras, "The effect of vortex pairing on particle dispersion and kinetic energy transfer in a two-phase turbulent shear layer," J. Fluid Mech. **302**, 149 (1995).